TURBOFAN INTERACTION NOISE REDUCTION USING TRAILING EDGE BLOWING: NUMERICAL DESIGN AND ASSESSMENT AND COMPARISON WITH EXPERIMENTS

Cyril Polacsek, Raphaël Barrier

ONERA, National Aerospace Research Agency, Châtillon, France

Michael Kohlhaas, Thomas Carolus

USI, Institute for Fluid and Thermodynamic, Siegen, Germany

Philip Kausche, Antoine Moreau

DLR, Berlin, Germany

Fritz Kennepohl

MTU Aero Engines, Munich, Germany

E-mail: cyril.polacsek@onera.fr

This paper investigates the effect of a flow control device on turbofan sound generation, applied to a low-speed axial compressor model in a laboratory test rig. This treatment consists in a secondary mass flow ejected through the trailing edge of the rotor blades, designed to fill the velocity defect behind the rotor and to decrease the turbulent kinetic energy related to the wakes, so that broadband interaction noise should be reduced. The design and implementation of the blowing device is first briefly described, as well as the fan stage experiment. Then the paper focuses on computation methods devoted to the capture of turbulent wakes and to the acoustic response of the stator (with and without blowing). 3D steady RANS and quasi-2D LES approaches are considered for the CFD, both coupled to an integral formulation based on Amiet's theory aiming at calculating the in-duct sound power and estimating the acoustic performance of the treatment. Under optimal blowing conditions, significant sound power reductions are predicted by the simulations. First attempts to relate numerical predictions to available measurements, i.e. hot-wire data and in-duct sound power spectra, are proposed and discussed.

Introduction

A major source of broadband turbofan noise results from the interaction of turbulent rotor blade wakes with the outlet guide vanes (OGV). The objective of the present study is to assess the effect of a flow control device on sound generation, applied to a low-speed axial compressor model in a laboratory test rig, and studied in the framework of the European project FLOCON. This treatment consists in a secondary mass flow ejected through the trailing edge of the rotor blades (Trailing Edge Blowing, TEB). It is designed to fill the velocity defect behind the rotor and to decrease the turbulent kinetic energy related to the wakes, so that interaction noise should be reduced. Tone noise reduction has been successfully investigated by Brookfield and Waitz[1] and Sutliff et al.[2], with optimal PWL tone reduction measured in the NASA Glenn Aero-Acoustic Propulsion Laboratory (AAPL) of 5.4, 10.6, and 12.4 dB for the first three tones, respectively. Further investigations of Sutliff[3] focused on broadband noise, showing a 2-3 dB average reduction on turbulent pressure

spectrum measured over stator vane surface. However, only 1 dB attenuation of broadband PWL in the aft arc was assessed by far-field measurements for optimal blowing rate, probably due to the rotor noise dominating contribution in the Advanced Noise Control Fan (ANCF) test bed. Noise benefits of rotor TE blowing have been also investigated on an advanced model turbofan tested in the NASA Glenn 9- by 15-Foot Low Speed Wind Tunnel (9x15 LSWT)[4], confirming the acoustic performance of the TEB for the tones and indicating some broadband noise reductions possibly attributed to a reduction of blade wake turbulence.

Another attempt is investigated here on a laboratory test rig with similar TEB technology and using extensive numerical simulations, focusing on the broadband noise component and only considering outlet duct acoustic measurements. Previous studies[5] showed that for most loaded OGV conditions, the broadband sound power measured in the outlet duct were mainly attributed to rotor-stator interaction mechanism. Compared to the 1.2 m diameter turbofan simulator used in [3], the present laboratory experiment is quite limited by the size of the rig (0.45 m rotor diameter) and then the thickness size of the vanes (very thin) at the trailing edge. Thus, practical blowing mass flow rates can only be reached by increasing the jet velocity. As pointed out in [6], the turbulent mixing of high-speed blowing jets can cause additional broadband noise sources that might increase the PWL spectrum (particularly the high-frequency part), as discussed in this paper too.

The design and implementing of the blowing device performed by USI (University of Siegen), already detailed in a more dedicated communication[7], is first briefly described here, as well as the fan stage experiment. Then the paper focuses on computation methods devoted to the capture of turbulent wakes and to the acoustic broadband response of the stator (with and without blowing). 3D steady RANS and quasi-2D LES approaches are considered for the CFD, both coupled to an integral formulation based on Amiet's theory aiming at calculating the in-duct sound power and estimating the acoustic performance of the treatment. Although restricted to a thin radial extent, LES permits to locally assess the turbulence spectrum content and the integral length scale. These methodologies and the resulting blowing effect on turbulence characteristics and acoustic behavior are addressed. First attempts to relate numerical predictions to available measurements, i.e. hot-wire data and in-duct sound power level (SPL) spectra are discussed.

Fan stage model and trailing edge blowing implementation

The measurements were performed in a laboratory scale fan rig located at DLR Berlin. For the design and the implementation of the blowing devices a new fan with 18 blades containing internal passages for TEB was designed. Important design parameters are given in Table 1 and Fig. 1. Two x-hot-wire probes located downstream of the rotor trailing edge plane are used to measure the wake characteristics and a microphone rake provides the acoustic spectra in the outlet duct.

Table 1. Design parameters of the fan stage

Volume flow rate at the inlet $\dot{V}_{in}$	2.52	[m^3/s]	Rotor speed, N	3159	[rpm]
Rotor diameter D_A	0.4524	[m]	Nr. of rotor blades, B	18	
Hub diameter D_I	0.286	[m]	Nr. of stator vanes, V	32	

For the rotor blade design, a NACA 6515-63 airfoil with span length L_{span} = 83.2 mm is used. The fan operates at its design flow rate coefficient:

$$\varphi_{in} \equiv \frac{\dot{V}_{in}}{\pi^2 D_A^3 N} = 0.21 \qquad (1)$$

The position of the reference plane corresponds to the stator leading edge. The wake velocity profiles and the turbulent quantities are evaluated at a relative blade height of

$$h^* \equiv \frac{h}{\left(D_A - D_I\right)/2} \quad . \tag{2}$$

As the circumferential velocity and hence the flow velocity around the blade increases from hub to tip, the wake deficit increases as well. This requires a spanwise distribution of the blowing parameters. For that each blade slot is divided into five discrete orifices which are fed separately via internal passages. The optimal blowing angle is determined by the orifice geometry and the flow angle of the wake deficit.

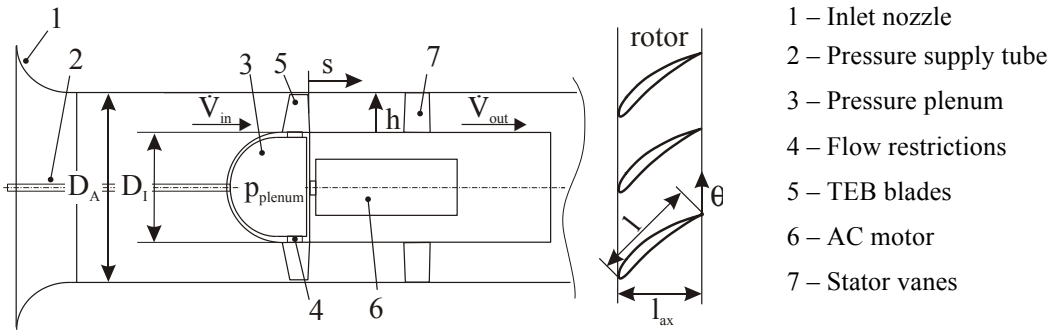

Figure 1. Schematic drawing of TEB fan stage: meridional cut (left) and coaxial section of cascade (right)

Fig. 2 shows the internal passages with guide vanes, shaped carefully to avoid excessive pressure losses. The internal passages responsible for a specific blade height are connected to the pressure plenum in the hub via flow restrictions which control the individual blowing mass flow rates. The inlet cross sections of the restrictions as well as the plenum pressure were optimized claiming at a flat wake velocity profile. A pressure supply tube from the inlet nozzle to the plenum delivers the needed pressure as well as the overall TEB mass flow.

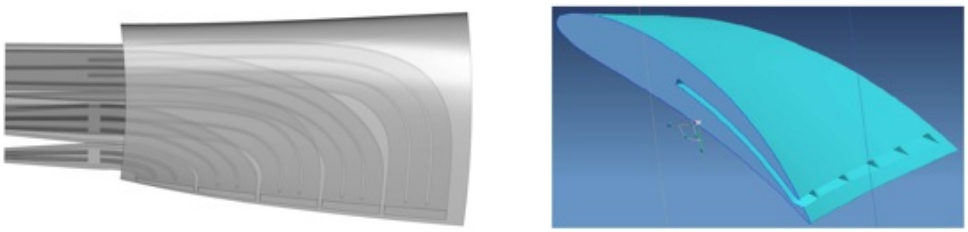

Figure 2. Rotor blade with internal passages, guide vanes and flow restrictors at the passage entrances (left), and CAD geometry (right) provided by USI

RANS-based and LES-based methodologies

3D RANS computations (USI)

RANS computations are mainly performed by USI. The computational domain consists of 1/18th of the bladed annulus from 1.0 D_A upstream to 1.0 D_A downstream of the rotor. It also covers the five internal blade passages including the guide vanes from their inlet in the hub to their orifices where the jet flow mixes with the main flow. General grid interface (GGI) boundary conditions were imposed in the circumferential direction. The inlet mass flow rate of the fan system was imposed on the upstream boundary according to the operation point of φ_{in}= 0.21, while an opening pressure boundary condition was set at the downstream boundary. At the entrance of each of the five internal blade passages the flow restrictions and the pressure plenum inside the hub were modeled. Of course no boundary conditions have to be specified at the channels exit (i.e. the orifices) since the flow mixes with the main flow. To solve the RANS equations, ANSYS CFX with the standard SST-turbulence model and a 2nd order approximation (blend factor of 1) was employed[8]. The block structured numerical grid consists of 7.1 million nodes. Special attention was paid to the wake region by using a very fine grid resolution of about 3 million nodes. Common grid quality criteria were considered in most of the fluid flow regions (grid angles > 20°). Due to

geometrical restrictions, some grid angles in the TEB injection orifices were as small as 13°. In these regions, a finer grid was employed to ensure sufficient accuracy. For the simulation, the maximum value of y^+_{max} for the first node adjacent to the blade surface was < 6, whereas the area averaged y^+_{ave} at the blade was < 1. The convergence criteria were set to $1 \cdot 10^{-6}$ MAX residuals.

3D RANS and quasi-2D LES computations (Onera)

3D RANS computations have been also performed on baseline case using the CFD Onera code elsA that solves the compressible equations in the relative frame with a cell-centered finite volume formulation. Space discretization is ensured using Jameson's second-order-centered scheme with the addition of an artificial viscosity. Turbulence closure is achieved using the $k-\ell$ turbulence model of Smith[9]. In this model, ℓ (characteristic length scale of turbulence) is a transported quantity. The computation is performed on a single rotor passage using a multi-block grid of about 1 million nodes. A particular attention has been paid to the mesh downstream of the blade to keep a good description along the wake development zone. The mesh has 17 cells in the rotor tip gap. Exit plane is located approximately at 3 chord lengths from the rotor trailing edge.

Due to CPU and memory limitations, LES approach is practically restricted to a quasi-2D computation[10,11] so that the simulation is only focused here on a thin strip (L_{strip}) of the full spanwise response. As done in Ref. 10, the sub-grid scale viscosity is given by the WALE model (Wall Adapting Local Eddy-viscosity)[12]. The quasi-2D computation domain is a cut in a circumferential plane at mid-span (corresponding precisely to half height of the central injection slit for the blowing case), and extruded in spanwise direction over 20% of the chord (Fig. 3, left). The full 3D test-case is thus converted to a cascade-like test-case for the LES simulation, assuming that flow physics of the fan rig remains well captured by this conversion. In the LES simulation, the incoming flow is perfectly laminar. Any "background" turbulence thus comes only from the unsteadiness created in the simulation (that is from shear, even small, outside the boundary layer and the wake zone). The mesh size (Δx, Δy, Δz) near the airfoil must verify some criteria for the validity of the LES computation. Non-dimensional criteria used for the present study are: $\Delta x^+ \leq 40$, $\Delta y^+ \leq 2$, $\Delta z^+ \leq 20$.

The blowing mass-flow in the central injection slit obtained from a 3D computation (USI) is translated in the quasi-2D LES as an equivalent mass-flow by using a uniform blowing along the whole extrusion of the blowing slit (Fig. 3, right). Optimal blowing conditions issued from USI computations were obtained with $\dot{m}_{blowing}$ = 142 g/s.

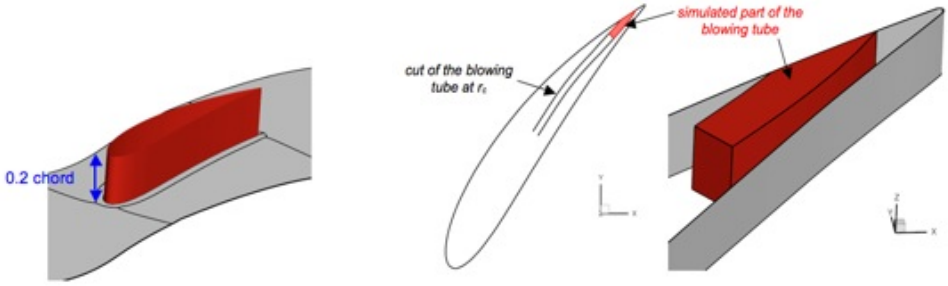

Figure 3. LES spanwise extrusion (left) and simulated part of the blowing tube (right)

Acoustic post-processing based on Amiet's broadband noise theory

This section presents the Amiet-based theory[13] adopted here in order to predict broadband interaction noise, using either 3D RANS or 2D LES output data. A concise form of Onera formulation[14] providing the power density spectrum (PSD) of the acoustic power, S_{ww}, in the outlet duct can be written as:

$$S_{ww}(f) = V \sum_{m=-m_{max}}^{+m_{max}} \sum_{n=1}^{n_{max}} \varphi_{mn}(r_s, f) \left| \mathcal{L}(r_s, K_c, 0) \right|^2 U_c \, \phi_{u_n u_n}(K_c, 0) \qquad (3)$$

φ_{mn} is a kernel function related to the Green's function (valid for an annular duct and a uniform mean flow), $\mathcal{L}$ is the aeroacoustic transfer function obtained from the aerodynamic response of an isolated (zero-thickness) stator vane. K_c and U_c are respectively the convection wave-number and the convection speed, taken equal to the streamwise velocity (U_s). $\phi_{u_n u_n}$ is the 2-wavenumber turbulence spectrum related to the upwash velocity component, u_n, and adjusted using standard Von-Karman model. $\phi_{u_n u_n}$ can be expressed versus the turbulent velocity spectrum, $S_{u_n u_n}$, and the spanwise correlation length scale, ℓ_y:

$$\phi_{u_n u_n}(K_c,0) = \frac{U_c}{\pi} S_{u_n u_n}(\omega)\,\ell_y(\omega) \tag{4}$$

$\phi_{u_n u_n}$ requires the knowledge of the mean-square turbulent velocity, u_{turb} (also related to the kinetic energy, k), and the integral length scale, Λ. These information are usually obtained from a RANS calculation. In Eq. (4), upwash turbulent velocity spectrum and spanwise correlation length scale might be directly post-processed from LES output data, as done here for $S_{u_n u_n}$. However, assessment of ℓ_y is practically not feasible, because the radial extent is too thin. An alternative approach is to use an analytical expression for ℓ_y deduced from the Von-Karman spectrum and directly related to Λ, as discussed by Lynch[15]. CFD data extraction for RANS and LES output post-processing is sketched in Fig. 4. Inter-stage red plane in Fig. 4 (left) corresponds to the hot-wire position in the DLR rig. Inputs to Eq. (4) are taken at stator leading edge (LE) position. In Fig. 4 (right), LES data are interpolated from the rotating frame to the fixed frame and uniformly distributed along mean streamline assumed to represent the path of convected turbulent structures impacting the stator vane (chord aligned to this path). This allows us to calculate the turbulent velocity spectra and the integral length scale at mid span.

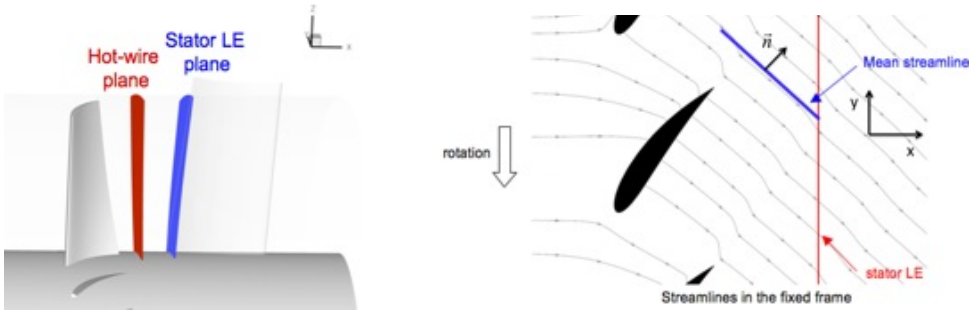

Figure 4. CFD data extraction for aeroacoustic analyses: 3D RANS (left) and quasi-2D LES (right)

Aerodynamic and noise predictions and comparison with experiment

Rotor wake characteristics

Firstly, wake characteristics in terms of velocity defect and turbulence intensity have been analyzed in order to check the reliability of the CFD computations (by comparison to the experiment on baseline case) and to estimate the effect of the blowing. Axial velocity profiles computed by USI RANS are compared to the measurements for two spanwise stations in Fig. 5. Predicted and measured blowing effects are similar, showing a significant reduction at 74% span but an overshoot at 44% span, revealing quite important radial effects. Although optimal blowing conditions assessed by RANS were estimated using a minimization process at several radial stations, wake filling performances achieved by a blowing distribution through the five slits and measured by the hot-wire probes reveal significant differences (compared to the simulations), particularly when moving towards the casing.

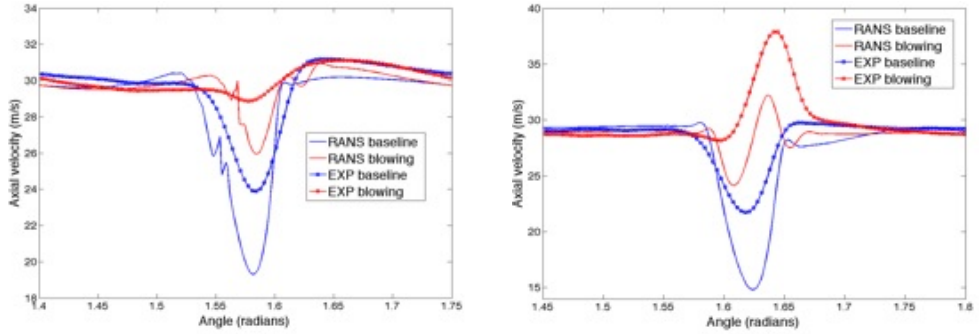

Figure 5. Axial velocity profiles issued from USI RANS and experiment at 74% (left) and 44% (right) span

Turbulence intensity, T_u , scaled by axial, radial and tangential velocity components is defined as:

$$T_u = \frac{u_{turb}^{1/2}}{U_s} = \frac{u_{turb}^{1/2}}{\sqrt{U_x^2 + U_r^2 + U_t^2}} \quad ; \quad u_{turb} = \frac{1}{3}\left(\left\langle u_x^2 \right\rangle + \left\langle u_r^2 \right\rangle + \left\langle u_t^2 \right\rangle\right) = \frac{2}{3}k \tag{5}$$

T_u 360°-plots issued from USI RANS baseline computation (1 rotor blade channel) and from baseline and blowing experimental cases (18 blade passages) are compared in Fig. 6. Agreement between prediction and measurements is rather good, although the turbulent wake level is over estimated by RANS. Intense turbulence spots near the hub and casing can be also observed in the experiments . Measured T_u wakes are clearly attenuated when the blowing is active (Fig. 6, right), despite of slight blade-to-blade irregularities. This effect is highlighted in Fig. 7 comparing the T_u plots over 1 blade channel (time-averaging using blade passing trigger in the experiment). The reduction of turbulence intensity due to the blowing is fairly well assessed by the CFD, but the levels are overpredicted, excepted near the blade foot region where the measurements are higher.

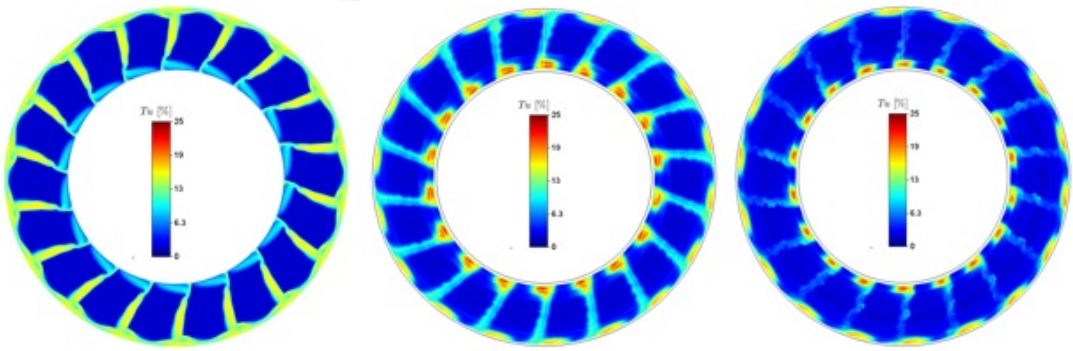

Figure 6. Turbulent intensity plots: RANS-SST (baseline, left) and exp. (baseline, mid. and blowing, right)

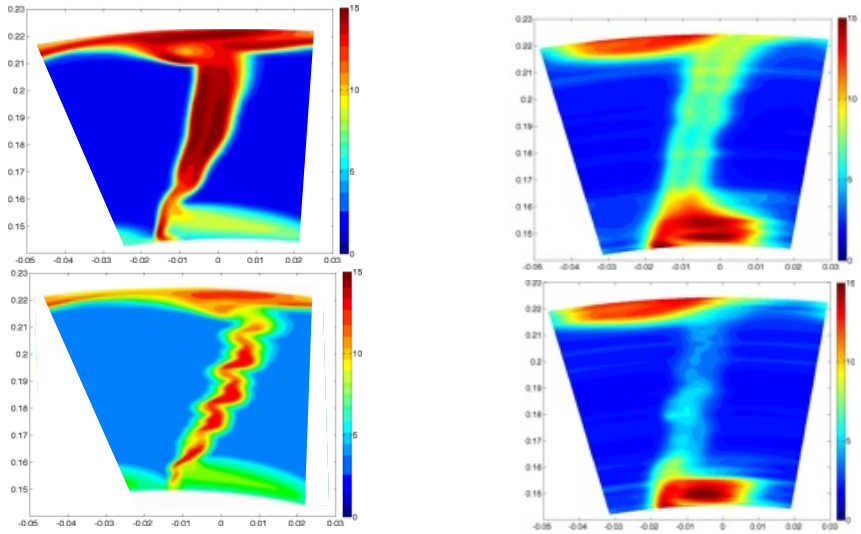

Figure 7. Blade channel turbulent intensity plots provided by RANS-SST (left) and experiment (right): baseline (top) and blowing (bottom) cases

The LES simulation is useful to capture unsteady phenomena as visualized in Fig. 8, showing a snapshot of Mach number and Q-criterion isosurface (with/without blowing). While both computations show a separation with production of turbulent structures occurring on the suction side of the blade, separation seems much less massive in the blowing case. Downstream the rotor, the turbulent structures are also smaller and restricted in a thinner wake when blowing is active. This phenomenon is highlighted in Fig. 9, related to the flow near the blowing slit obtained by an average of LES solution during five rotor blade passage, which reveals a strong blowing effect that tends to delay the separation and reattachment points of the boundary layer almost up to the blowing slit. The turbulence kinetic energy in the blade wake region computed from velocity fluctuations during five rotor blade passage is plotted in Fig. 10, for baseline and blowing cases. A strong reduction of the turbulence kinetic energy can be clearly seen when the blowing is active.

These LES predictions were carefully checked by comparing the relevant averaged fields to those provided by RANS at same spanwise position. Angular profiles of turbulence intensity deduced from LES (with/without blowing) at inter-stage position are plotted in Fig. 11 and compared to the RANS $k-\ell$ baseline solution. T_u is strongly reduced by the blowing and baseline solutions are found to be rather close to experiment with an LES amplification that could be attributed to confined grid (quasi-2D) effects. One should note that the background turbulence level (about 2%) visible in Fig. 11 is contributing to the theta-averaged levels of T_u profiles discussed below. For reliability, we tried to get similar value of this background turbulence level between RANS and measurements at the inlet boundary condition, as shown by the comparison addressed in Fig. 12.

Finally, the radial profiles of T_u obtained from a circumferential averaging of CFD solutions at hot-wire plane are compared to experiment (blade passage trigger average) on baseline case in Fig. 13, showing best agreement for the RANS-SST model. Blowing efficiency provided by USI RANS is found comparable to the measurements in terms of T_u reduction (Fig. 13, right). As already observed in Figs 6 and 7, a strong turbulence activity is measured in the vicinity of the hub, attributed to a flow separation near the blade foot (laboratory test rig imperfections) and giving rise to vortices shedding not captured by RANS, and not reduced by the blowing.

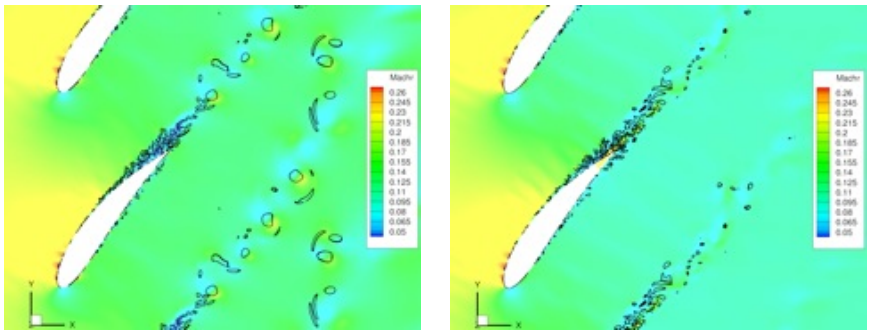

Figure 8. Relative Mach number and iso-surface of Q-criterion (LES snapshot): Baseline case, left and blowing case, right

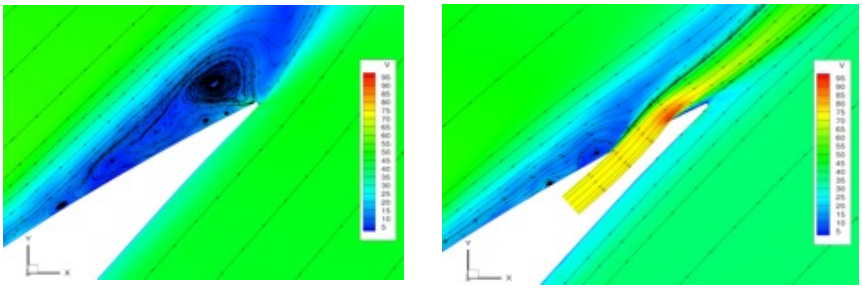

Figure 9. LES-averaged relative velocity amplitude and streamlines near the blowing slit without (left) and with (right) blowing

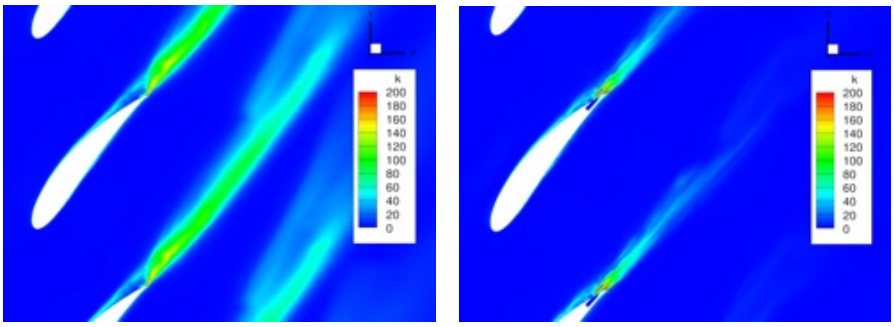

Figure 10. Turbulence kinetic energy (m²/s²) from LES velocity fluctuations averaging: Baseline case, left and blowing case, right

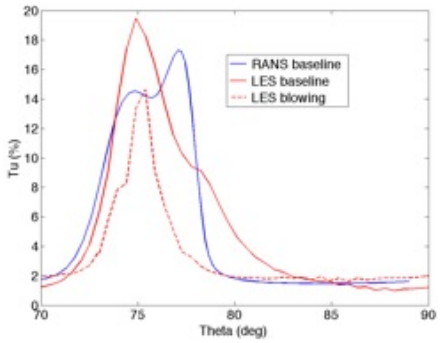

Figure 11. LES T_u profiles compared to RANS k-ℓ at mid-span and hot-wire axial position

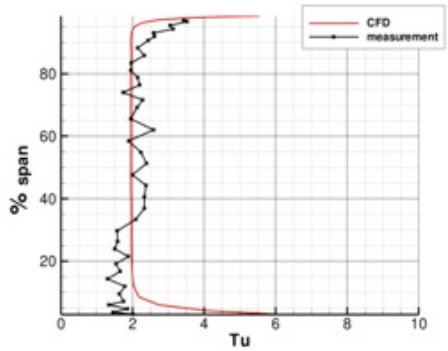

Figure 12. T_u intensity (%) provided by RANS k-ℓ compared to measurement in the inlet

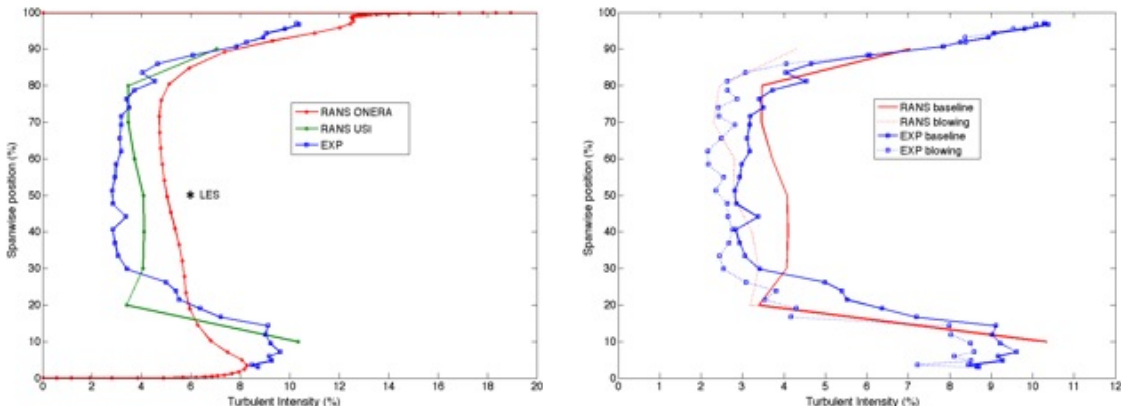

Figure 13. T_u radial profiles: CFD vs. experiment on baseline case (left) and blowing vs. baseline (right)

Turbulent velocity spectra and correlation scales

LES simulation data are post-processed in order to assess the turbulent velocity spectra and correlation scales. PSD of upwash velocity component ($S_{u_n u_n}$ in Eq. (4)) calculated at inter-stage for baseline and blowing cases are compared in Fig. 14 to the Von-Karman spectra (used in Eq. (3)). Slopes are similar, but a hump over a wide frequency range can be observed in the LES solutions. The streamwise 0-time shift cross-correlation function (applied to the streamwise velocity component) is compared for baseline case to the theoretical Gaussian solution[11] in Fig. 15 left, showing a very good agreement. The integral scale Λ (deduced by integration over x) is found to be close (at mid-span) to the RANS-based solutions plotted Fig. 15 right. RANS-based solutions are issued from a circumferentially average of the integral length scale, directly extracted from the CFD for Onera result, because this length is a transported quantity of the $k-\ell$ turbulence model. Turbulent (streamwise) velocity spectra measured by hot-wire probes at 74% and 44% span are

plotted in Fig. 16 left and right, respectively. These are compared to the LES solution scaled in level (- 10 dB) and over plotted in Fig. 16 left, showing very close attenuation slopes and similar trends of blowing effects at 74%. However, blowing at 44% is much less efficient with a level increase for frequencies beyond 4 kHz. Thus the OASPL obtained with blowing for this radial station would be just slightly lower than the baseline case. A similar tendency for measured turbulence intensity profiles can be observed in Fig. 13, showing a lower level reduction around 45% span (discarding the spurious baseline oscillating point) compared to 75% span. The rise of turbulent velocity levels beyond 4 kHz (Fig. 16 right) should have a hard impact on the noise level in this frequency range, as it will be discussed in next section. One should note also the numerous peaks visible in the red spectra when the blowing is active (whereas only expected BPF tones are present without blowing). These might be attributed to small blowing jet variations from blade-to-blade (non-homogeneous wake filling) giving rise to multiple pure tones (rotor rotation harmonics). Such extra tones were pointed out in Ref. 4 when investigating alternate blade blowing.

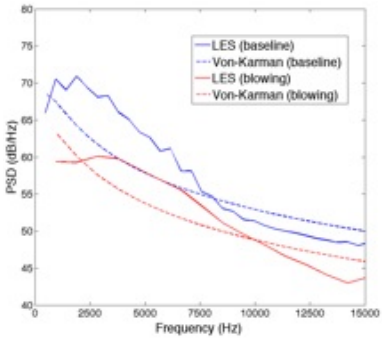

Figure 14. PSD of upwash turbulent velocity issued from LES and Von-Karman model

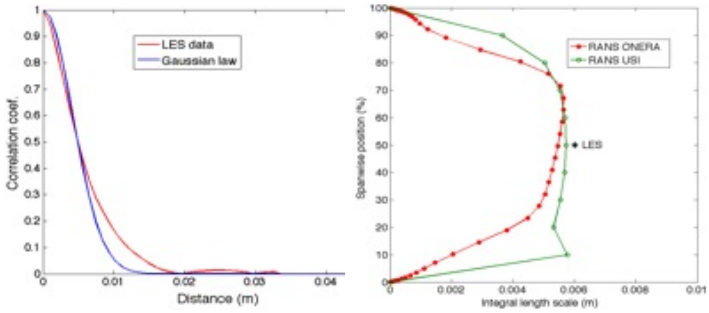

Figure 15. LES-based streamwise correlation function (left) and integral length scales deduced from RANS and LES (right)

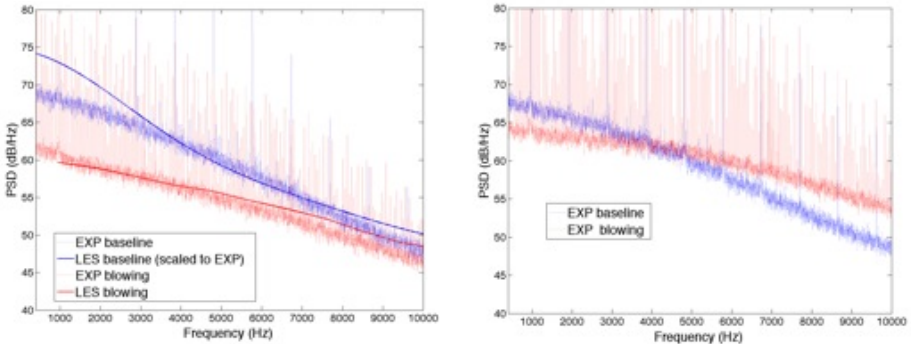

Figure 16. PSD of streamwise turbulent velocity at 74% span (left) and at 44% span (right)

Assessment of sound power level broadband noise reduction

Previous RANS and LES analyses are used to estimate the PSD of acoustic pressure in the outlet duct (observer at outer wall), as shown in Fig. 17 for the baseline case. The LES-based prediction is achieved by applying a basic scaling correction $10\log\left(L_{span}/L_{strip}\right)$ on the sound pressure level (SPL). A satisfactory agreement is obtained for the RANS-based solutions, whereas the LES-based spectrum is over-predicted (certainly due to the quasi-2D approach restrictions). However, the frequency slope using LES seems better appraised. Finally, PSD of acoustic power (PWL spectra) using RANS-SST and LES input data are presented and compared in Fig. 18 left. Sound power (obtained by integrating acoustic intensity along the duct section) is more suited than sound pressure to estimate the acoustic performance of the TEB, and calculated PWL spectra have been smoothed for clarity. As expected from turbulent wake analyses, significant reductions are observed in the computation results with relative level attenuations that are twice for LES compared to RANS (about 7 dB vs. 3.5 dB max), but with quite similar behavior with respect to frequency.

This has to be related to the experimental SPL spectra, measured by a microphone at casing wall, in Fig. 18 right. Unfortunately, experimental results do not display any noise reduction, neither for the tones (see the non-filtered spectra), and even more highlight a broadband level increase for frequencies beyond 4 kHz. This sound increase at high frequencies is certainly related to the rise of turbulent velocity spectra already observed from the hot-wire probe results at 44% span (Fig. 16 right). This is quite disappointing as numerical simulations suggested significant acoustic performances of the present TE blowing device, confirming the previous published results from Nasa Glenn tests[3,4]. A few possible explanations of this test failure are addressed in the last section.

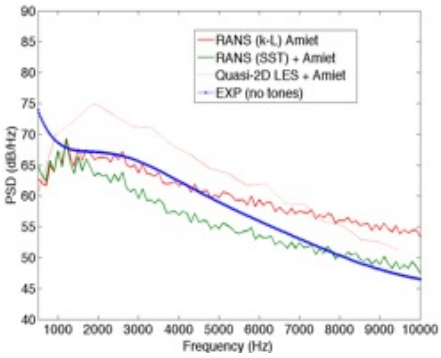

Figure 17. SPL spectra (baseline) issued from calculations and experiment

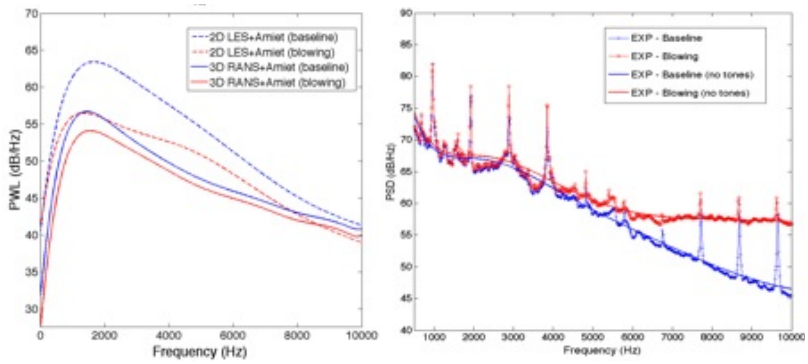

Figure 18. Blowing effect on broadband noise spectra PWL predictions (smoothed, left) and SPL measurements (right)

Possible explanations of noise reduction failure in the experiments

Regarding to CFD data and hot-wire probe analyzes, three main reasons for observing no noise reduction in the experiments can be argued:

- The present laboratory axial compressor rig is characterized by intense turbulence structures in the vicinity of the hub and the casing that largely contribute to the RSI broadband noise and that are poorly impacted by the blowing. The blowing mass flow rate was optimized assuming no separated flows at the blade foot and thus under-predicting these 3D effects in the spanwise direction. TE blowing in this test rig is certainly efficient with respect to turbulent wake reduction away from these regions. This decrease of turbulent wake intensity is balanced by the interaction sources in near the hub and casing. Similar spanwise dependency has been noticed for the velocity defects (reduction at 75% and overshoot at 45% span), limiting the tone noise reduction too;
- A non-homogeneous wake filling from blade-to-blade is suspected from rotor-clock average analyzes, revealing non fully periodic wakes in the (r-θ) planes and the presence of numerous tones in the hot-wire spectra when the blowing is active. This might be also responsible for minimizing the efficiency of the blowing assumed to be fully homogeneous in the simulations ;
- Due to the small size of the slits, blowing jet speed is very high, and jet mixing velocity fluctuations captured by hot-wire measurements at some radial positions might contribute to self jet noise, particularly at medium and high frequencies, as displayed by the sound spectra.

Conclusions

A comprehensive study of turbofan broadband noise reduction using a trailing edge blowing device has been carried out numerically and experimentally in a laboratory axial compressor stage rig. The blowing design and optimal settings were obtained through extensive RANS computational studies. 3D RANS simulations have been supplemented by quasi-2D LES in order to better assess the turbulent characteristics of the flow, and CFD post-processed data have been used as input to an Amiet-based acoustic calculation. Wake analyses have shown relevant reductions of velocity defect and turbulent intensity, in good agreement with the hot-wire measurements performed in the inter-stage plane. These are responsible for significant SPL attenuations in the outlet duct spectra (up to

3.5 dB for RANS-based and up to 7 dB for LES-based solutions) with a similar response to frequency, which lets the present methodology appear reliable. However, the acoustic measurements have not revealed any acoustic performance of the blowing (even more some noise increase was detected at high frequencies). This mismatch has been discussed at the end of the paper and can be attributed to a strong turbulence activity in the test rig duct walls hub and to a non-homogeneous wake filling from blade-to-blade. Contribution of mixing jet sources not considered in the present simulations is also suspected.

Acknowledgements. This work was supported by European Commission (FLOCON).

References

1 Brookfield, J. M., Waitz, I. A, *Trailing-Edge Blowing for Reduction of Turbomachinery Fan Noise*, Journal of Propulsion and Power, Vol. 16, No. 1, pp. 57-64, 2000.

2 Sutliff, D. L., Tweedt, D. L., Fite, E. B., and Envia, E., *Low Speed Fan Noise Reduction with Trailing Edge Blowing*, NASA/TM-2002-211559, 2002.

3 Sutliff, D. L., *Broadband Noise Reduction of a Low-Speed Fan Noise Using Trailing Edge Blowing*, NASA/TM-2005-213814 and AIAA-2005-3028, 2005.

4 Woodmark R. P., Fite E. B., and Podboy, G. G., *Noise Benefits of Rotor Trailing Edge Blowing for a Model Turbofan*, AIAA-2007-1241, 2007.

5 Jurdic, V., Moreau, A., Joseph, P., Engardt, L., and Coupland, J., "*A comparison between measured and predicted fan broadband noise due to rotor-stator interaction*," AIAA-2007-3692, 2007.

6 Langford, M. L., Minton, C., Ng, W. F., Burdisso, R. A., and Halasz, C., *Fan Flow Control for Noise Reduction Part 3: Rig Testing of Optimal Design*, AIAA-2005-3027, 2005.

7 Kohlhaas, M., Carolus, T., *Trailing Edge Blowing for Reduction of Rotor-Stator Interaction Noise: Criteria, Design and Measurements*, ISROMAC-14, Honolulu (USA), 2012.

8 Ansys, *Ansys CFX-Solver, Release 10.0: Modelling*, Canonsburg, Pennsylvania., 2005.

9 Smith, B. R., *The Near-Wall Model for the k-l Two Equation Turbulence Model,* AIAA-94-2386, 25th Fluid Dynamics Conference, Colorado Springs (Colorado), 1994.

10 Riou, J., Léwy, S. and Heib, S., *Large Eddy Simulation for predicting rotor-stator broadband interaction fan noise,* Inter-noise 2007, Istambul, August 2007.

11 Ashcroft G., Nurnberger, D., *A computational investigation of broadband noise generation in a low-speed axial fan*, AIAA-2009-3219, Miami (Florida), 2009.

12 Nicoud, F., Ducors, F., *Subgrid-scale stress modelling based on the square of the velocity gradient*, Flow Turbulence and Combustion, Vol. 62(3), pp. 183-200, 1999.

13 R. K. Amiet, R. K., *High-frequency thin airfoil theory for subsonic flow*, AIAA Journal, **14**(8), 1976.

14 Reboul, G., Polacsek, C., Léwy, S. and Heib, S., *Ducted-fan Broadband Noise Simulations Using Unsteady or Averaged Data*, Inter-noise2008, Shangaï (China), 2008.

15 Lynch, D.A., Mueller, T.J., and Blake, W.K., *A Correlation Length Scale for the Prediction of Aeroacoustic Response*, AIAA-2002-2569, 2002.

Authors

Cyril Polacsek graduated from Ecole Nationale Supérieure d'Ingénieurs de Poitiers (ENSIP) in 1989, combined with a Masters Degree in aeroacoustics and signal processing. He started his carrier at ONERA as a test engineer (rotorcraft test campains in S1-Modane wind tunnel facilities), and became a specialist in source modeling and numerical simulations related to turbomachinery noise. He is now in charge of turbofan noise activities in the « CFD and Aeroacoustics » Department.

Raphaël Barrier graduated from École Centrale de Marseille and received a Masters Degree in mechanical and aerospace engineering at Ecole Centrale Paris in 2005. Engineer at Onera since 2006, he is in charge of CFD studies and software development concerning analysis and design for turbomachinery components. He is also the technical and scientific responsible of the turbomachinery related studies in the Applied Aerodynamics Department.

Michael Kohlhaas graduated in 2009 from the University of Siegen where he obtained his Diploma degree in Mechanical Engineering. Since 2009, he works as a doctoral student in the Turbomachinery Group of the Institute of Fluid- and Thermodynamic (IFT) in Siegen. His current activities involve the reduction of rotor-stator interaction noise by trailing edge blowing.

Prof. Thomas Carolus is head of the Turbomachinery Group in the Institute of Fluid- and Thermodynamic (IFT) at the University of Siegen, Germany. He received his Diploma, Master and Ph.D. degrees from the Universität (Technische Hochschule) Karlsruhe and the Georgia Institute of Technology in Atlanta, USA. Before joining the University of Siegen he was senior research engineer at the German automotive supplier Bosch.

Philip Kausche studied Aeronautics and Astronautics at the Technical University of Berlin and graduated in 2008. He wrote his diploma thesis at the department of Engine Acoustics at the German Aerospace Center (DLR) in Berlin. Since then, he worked there as a research scientist on several European projects. Currently he works on the completion of his dissertation, which is about noise control in a turbomachine.

Antoine Moreau studied in Toulouse at the Ecole Nationale Supérieure d'Ingénieurs en Construction Aéronautique (ENSICA) and obtained his degree in Aerospace Engineering in 2005. Since then, he has been working at the Engine Acoustics Department of the German Aerospace Center (DLR) located in Berlin.
His research is focused on fan and compressor acoustics and the development of low-noise aerodynamically efficient designs, based on experiments and theoretical prediction methods.

Fritz Kennepohl received his mechanical engineering diploma at Technical University of Braunschweig in 1978. Since then he has been working for MTU Aero Engines in various positions on acoustic design of aeroengine components, development of noise prediction methods, analysis of measurements etc. His scientific focus has been on generation and reduction of turbomachinery noise and particularly turbine noise. He retired in 2013, after the end of the European Research project FLOCON.